Author Manuscript

Author Manuscript

Author Manuscript

Author Manuscript

HHS Public Access

Author manuscript

Cell. Author manuscript; available in PMC 2017 June 30.

Published in final edited form as:

Cell. 2016 June 30; 166(1): 88–101. doi:10.1016/j.cell.2016.05.034.

Digestion of Chromatin in Apoptotic Cell Microparticles Prevents Autoimmunity

Vanja Sisirak[1,12], **Benjamin Sally**[1,2,12], **Vivette D'Agati**[3], **Wilnelly Martinez-Ortiz**[4], **Z. Birsin Özçakar**[5], **Joseph David**[1], **Ali Rashidfarrokhi**[1], **Ada Yeste**[6], **Casandra Panea**[2], **Asiya Seema Chida**[7], **Milena Bogunovic**[8], **Ivaylo I. Ivanov**[2], **Francisco J. Quintana**[6], **Inaki Sanz**[7], **Keith B. Elkon**[9], **Mustafa Tekin**[10], **Fatoş Yalçınkaya**[5], **Timothy J. Cardozo**[4], **Robert M. Clancy**[11], **Jill P. Buyon**[11], and **Boris Reizis**[1,2,11,*]

[1]Department of Pathology, New York University School of Medicine, New York, NY 10016, USA

[2]Department of Microbiology and Immunology, Columbia University Medical Center, New York, NY 10032, USA

[3]Department of Pathology, Columbia University Medical Center, New York, NY 10032, USA

[4]Department of Biochemistry and Molecular Pharmacology, New York University School of Medicine, New York, NY 10016, USA

[5]Division of Pediatric Nephrology, Department of Pediatrics, School of Medicine, Ankara University, Ankara, 06100, Turkey

[6]Ann Romney Center for Neurologic Diseases, Brigham and Women's Hospital, Harvard Medical School, Boston, MA 02115, USA

[7]Division of Rheumatology, Department of Medicine, Emory University, Atlanta, GA 30322, USA

[8]Department of Microbiology and Immunology, Milton S. Hershey Medical Center, Pennsylvania State University, Hershey, PA 17033, USA

[9]Department of Medicine, University of Washington, Seattle, WA 98195, USA

[10]Department of Human Genetics, Miller School of Medicine, University of Miami, Miami, FL 33136, USA

[11]Department of Medicine, New York University School of Medicine, New York, NY 10016, USA

SUMMARY

[*]Correspondence: boris.reizis@nyumc.orghttp://dx.doi.org/10.1016/j.cell.2016.05.034.

[12]Co-first author

SUPPLEMENTAL INFORMATION

Supplemental Information includes Supplemental Experimental Procedures and seven figures and can be found with this article online at http://dx.doi.org/10.1016/j.cell.2016.05.034.

AUTHOR CONTRIBUTIONS

V.S., B.S., V.D., W. M.-O., J.D., A.R., and A.Y. performed and interpreted the experiments. F.J.Q., T.J.C., R.M.C, J.P.B., and B.R. supervised and interpreted the experiments. Z.B.O., C.P., A.S.C., M.B., I.I.I., I.S., M.T., F.Y., K.B.E., R.M.C., and J.P.B. provided samples and reagents. K.B.E., R.M.C., and J.P.B. provided advice and feedback. B.R. conceived and supervised the project. V.S. and B.R. wrote the manuscript.

Author Manuscript Author Manuscript Author Manuscript Author Manuscript

Antibodies to DNA and chromatin drive autoimmunity in systemic lupus erythematosus (SLE). Null mutations and hypomorphic variants of the secreted deoxyribonuclease DNASE1L3 are linked to familial and sporadic SLE, respectively. We report that DNASE1L3-deficient mice rapidly develop autoantibodies to DNA and chromatin, followed by an SLE-like disease. Circulating DNASE1L3 is produced by dendritic cells and macrophages, and its levels inversely correlate with anti-DNA antibody response. DNASE1L3 is uniquely capable of digesting chromatin in microparticles released from apoptotic cells. Accordingly, DNASE1L3-deficient mice and human patients have elevated DNA levels in plasma, particularly in circulating microparticles. Murine and human autoantibody clones and serum antibodies from human SLE patients bind to DNASE1L3-sensitive chromatin on the surface of microparticles. Thus, extracellular micro-particle-associated chromatin is a potential self-antigen normally digested by circulating DNASE1L3. The loss of this tolerance mechanismcan contribute to SLE, and its restoration may represent a therapeutic opportunity in the disease.

Graphical abstract

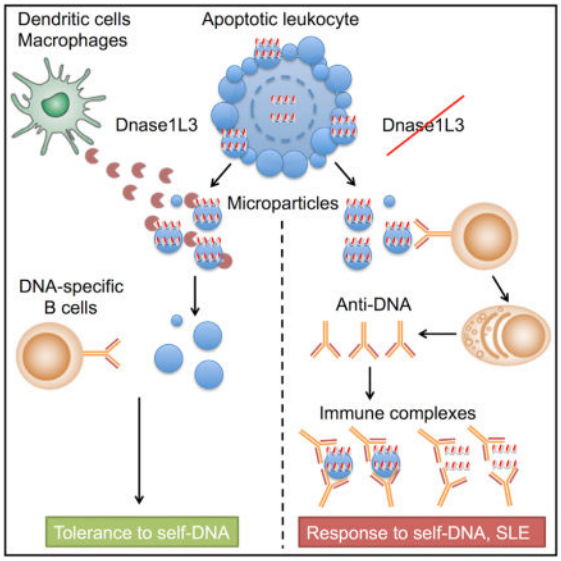

INTRODUCTION

The hallmark of systemic lupus erythematosus (SLE) is the production of antibodies (Abs) to nuclear antigens, such as ribonucleoproteins and DNA. Auto-Ab production by self-reactive B cells triggers and is further amplified by the activation of the innate immune system, including myeloid cell activation and secretion of type I interferon (interferon α/β; IFN) (Choi et al., 2012). Ultimately, auto-Abs forming immune complexes with nucleic acids are deposited in tissues, where they cause chronic inflammation, such as vasculitis and glomerulonephritis. High-affinity immunoglobulin G (IgG) Abs to double-stranded DNA (dsDNA) are particularly pathogenic and associated with the severity of clinical disease in SLE (Pisetsky, 2016). Furthermore, Abs to chromatin, including nucleosomes, are common in SLE and may serve as especially sensitive biomarkers of the disease (Rekvig et al., 2014).

Author Manuscript Author Manuscript Author Manuscript Author Manuscript

Thus, the loss of B cell tolerance to DNA and/or chromatin represents a major mechanism of SLE pathogenesis.

DNA-reactive antigen receptors are present in the normal B cell repertoire (Wardemann and Nussenzweig, 2007). Therefore, a major question of SLE pathogenesis concerns the physical form(s) of DNA that can be recognized by autoreactive B cells and the mechanisms that normally prevent such recognition. DNA from apoptotic cells is degraded by the intracellular enzyme DNASE2, whose deletion in mice causes IFN-driven autoinflammation (Nagata and Kawane, 2011). Similarly, DNA of reverse-transcribed retroelements is degraded by an intracellular exonuclease TREX1, and the loss of TREX1 causes IFN-driven inflammatory disease in human patients (Aicardi-Goutieres syndrome) and in mice (Crow, 2015; Volkman and Stetson, 2014). Importantly, these inflammatory conditions are driven by innate DNA sensing that requires the cytoplasmic protein STING (Ahn et al., 2012; Gall et al., 2012). Other potentially immunogenic forms of DNA are neutrophil extracellular traps (NETs) and oxidized mitochondrial DNA released by activated granulocytes (Caielli et al., 2016; Lood et al., 2016). These stimuli may engage endosomal Toll-like receptor (TLR) TLR9 or STING to induce IFN production, yet their role as B cell antigens remains unclear. Finally, genomic DNA of apoptotic cells is incorporated into membrane-coated microparticles (Pisetsky et al., 2011), which are normally present in the plasma of healthy subjects and SLE patients (Dieker et al., 2016; Nielsen et al., 2011, 2012). These microparticles (MP) were shown to expose chromatin on their surface (Ullal et al., 2011, 2014) and therefore may represent antigens for DNA-reactive B cells. However, the relationship of MP DNA to total DNA in human plasma (Snyder et al., 2016; Sun et al., 2015), the regulation of MP DNA, and potential role for MP DNA in SLE remain obscure.

A recent study (Al-Mayouf et al., 2011) identified several families with a high incidence of aggressive SLE with anti-dsDNA reactivity in children. The phenotype segregated with homozygosity for the same frameshift mutation in the *DNASE1L3* gene. A subsequent study (Ozçakar et al., 2013) identified independent *DNASE1L3* mutations in two families with autosomal-recessive hypocomplementemic urticarial vasculitis syndrome (HUVS). HUVS is often associated with SLE, and indeed 3 out of 4 surviving *DNASE1L3*-deficient children developed severe SLE with anti-dsDNA. Furthermore, previously described associations of *PXK* gene with sporadic SLE and a related systemic autoimmune disease scleroderma (Martin et al., 2013) have been reassigned to the adjacent *DNASE1L3* gene (Mayes et al., 2014; Zochling et al., 2014). The disease-associated *DNASE1L3* polymorphism (*rs35677470*) creates an amino acid substitution (R206C) that reduces DNase activity (Ueki et al., 2009). Collectively, these data establish DNASE1L3 as a genetic determinant of SLE susceptibility and an essential factor protecting humans from the disease.

DNASE1L3 is homologous to DNASE1, a secreted DNase that digests DNA in the gastrointestinal tract (Baron et al., 1998). DNASE1 and DNASE1L3 together are responsible for the DNase activity in serum (Napirei et al., 2009). However, unlike DNASE1 or its other homologs, DNASE1L3 contains a short, positively charged C-terminal peptide that allows it to digest DNA encapsulated into liposomes (Wilber et al., 2002). In addition, DNASE1L3 is more efficient than DNASE1 in the internucleosomal cleavage of genomic DNA in isolated cell nuclei (Napirei et al., 2005), suggesting that it might digest chromatin within apoptotic

Author Manuscript Author Manuscript Author Manuscript Author Manuscript

or necrotic cells (Mizuta et al., 2013). However, neither the natural form of DNA targeted by DNASE1L3 nor the mechanism whereby DNASE1L3 protects from SLE has been elucidated.

Here, we show that the loss of DNASE1L3 in mice caused a rapid Ab response to dsDNA and chromatin. We also found that DNASE1L3 is capable of digesting chromatin in apoptotic cell-derived MP, and its absence caused the accumulation of and Ab response to micro-particle-associated DNA. These results suggest that chromatin in apoptotic MP represents an important antigenic form of DNA in SLE and identifies DNASE1L3 as a regulator of this antigenic chromatin's ability in the steady state.

RESULTS

Dnase1l3-Deficient Mice Rapidly Develop Anti-DNA Auto-Abs

We analyzed mice in which essential coding exons of the *Dnase1l3* gene have been replaced with a *LacZ* reporter cassette (Figure S1A). The *Dnase1l3*^{LacZ} allele was crossed onto two common inbred backgrounds, C57BL/6 (B6) and 129SvEv (129). Homozygous *Dnase1l3*$^{LacZ/LacZ}$ knockout (KO) mice were born at Mendelian ratios and were grossly normal and fertile. All KO mice on both B6 and 129 backgrounds developed anti-nuclear Abs (ANA) with perinuclear staining (Figure 1A), which is characteristic of severe human SLE. Anti-dsDNA IgG in the sera of KO mice were elevated at 5 weeks and progressively increased with age (Figure 1B). Both male and female KO mice developed anti-dsDNA with the same kinetics (data not shown). Anti-dsDNA primarily comprised IgG2a and IgG2b isotypes pathogenic in other SLE models (Ehlers et al., 2006) (Figure 1C). ELISPOT analysis showed that anti-dsDNAIgG Ab-secreting cells (ASC) were abundant in KO spleens and detectable as early as 4–6 weeks of age (Figures 1D and 1E). In contrast, neither total IgG nor anti-RNA IgG were elevated, even in old mice (Figures S1B and S1C). The analysis ofKOsera by autoantigen microarrayandELISA revealed increased reactivity to several protein andribonucleoprotein auto-antigens at 40 weeks, but not earlier (Figures S1D–S1F).

To test Ab response to chromatin, we tested IgG reactive with native-purified polynucleosomes. KO mice rapidly developed high titers of anti-chromatin IgG on both 129 and B6 backgrounds (Figure 1F; data not shown). No reactivity to purified histones was observed (data not shown). The analysis of a synchronized cohort of KO mice showed that anti-chromatin IgG developed even more rapidly than anti-dsDNA IgG at 5 weeks (Figures 1G and 1H). Thus, *Dnase1l3*-deficient mice manifest rapid and specific responses to dsDNA and chromatin, suggesting that the endogenous genomic DNA represents the primary autoantigen in this model.

Dnase1l3-Deficient Mice Develop Features of SLE

Peripheral blood of KO mice harbored a progressively increasing fraction of CD11c^{+} MHC class II^{-} CD11b^{+} Ly-6C^{-} monocytes (Figures 2A and 2B), which correspond to Gr1^{-} monocytes expanded in other SLE models (Santiago-Raber et al., 2009). By 50 weeks of age, KO mice manifested splenomegaly (Figures 2C and 2D) with reduced marginal zone B

Author Manuscript Author Manuscript Author Manuscript Author Manuscript

(MZB) cell population and increased fractions of monocytes and activated T cells (Figures S2A–S2C). The enlarged spleens showed spontaneous germinal center (GC) formation and an increased fraction of GC B cells (significant on the 129 background; Figures 2E and 2F). All 50-week-old KO mice on both backgrounds showed IgG deposition in the kidney glomeruli (Figure 2G). Finally, KO mice on the 129 background developed glomerulonephritis, including enlargement of glomeruli, mesangial and endocapillary proliferation, glomerular deposits, and interstitial inflammation of the kidney cortex (Figures 2H and 2I). KO mice on the B6 background showed glomerular enlargement, but no overt glomerulonephritis. Thus, anti-DNA response in *Dnase1l3*-deficient mice is followed by immune activation, IgG deposition, and a background-dependent glomerulonephritis.

Despite the early onset of the anti-DNA response, the observed immune activation was largely absent from KO mice up to 27 weeks of age (Figures 2D, 2E, and S2A–S2C). The development of experimental SLE can be accelerated by a surge in IFN production, e.g., after the adenoviral delivery of IFN (Mathian et al., 2005). We injected young KO or control mice with the adenoviral vector encoding IFN-α5, resulting in elevated serum IFN and elevated expression of IFN-inducible protein Sca-1 for at least 5 weeks post-injection (Figures S2D and S2E). IFN-treated KO mice showed rapid accrual of anti-dsDNA IgG (Figure S2F), as well as the appearance of anti-RNA IgG (Figure S2G). Furthermore, IFN-treated KO mice showed monocyte expansion and T cell activation as early as 1 week post-injection (Figures S2H and S2I), and two-thirds of these mice died after 35 weeks (Figure S2J). Therefore, immune activation in KO mice can be accelerated by IFN expression, recapitulating severe SLE in *DNASE1L3*-deficient human patients.

Circulating Dnase1l3 Protects from Autoreactivity

If DNASE1L3 acts similarly to DNASE2 or TREX1 as proposed (Ghodke-Puranik and Niewold, 2015; Picard et al., 2015), autoreactivity in KO mice should involve intracellular DNA accumulation and sensing through STING. However, the deletion of STING did not diminish ANA, anti-dsDNA IgG and ASC, IgG deposition (Figures 3A–3D), or splenomegaly (Figure S3A) in KO mice. The median anti-dsDNA titers were increased in DNASE1L3/STING double-deficient KO mice, although not significantly (Figure 3B). In contrast, all these manifestations were completely abolished by the deletion of MyD88, the transducer of TLR and IL-1 receptor signals (Figures 3A–3D and S3A). These data suggest that DNASE1L3 does not target DNA within cells, consistent with the secreted nature of this DNase.

We detected circulating DNASE1L3 in mouse serum using the digestion of liposome-coated plasmid DNA as a readout (Figure 3E). We then set up reciprocal bone marrow (BM) transfers between wild-type (WT) and KO mice and measured serum DNASE1L3 activity over time. The KO→WT and WT→KO chimeras showed progressive loss and gain of serum DNASE1L3, respectively (Figure S3B), suggesting that circulating DNASE1L3 is produced by hematopoietic cells. Importantly, the loss of circulating DNASE1L3 in KO→WT chimeras led to the development of anti-dsDNAASC (Figure S3C). In a cohort of KO→WT chimeras in which DNASE1L3 activity disappeared by 40 weeks post-transfer (Figure 3F), anti-dsDNA IgG appeared at the same time point (Figure 3G), eventually

Author Manuscript Author Manuscript Author Manuscript Author Manuscript

leading to ANA, IgG deposition, glomerular enlargement, and mild glomerulonephritis (Figures S3D–S3G). Thus, autoreactivity in *Dnase1l3*-deficient mice inversely correlates with circulating DNASE1L3 produced by hematopoietic cells.

To directly test the effect of circulating DNASE1L3 on autoreactivity, we injected young KO mice with an adenoviral vector-encoding human DNASE1L3 (Ad-DNASE1L3). Adenoviral vectors in vivo transduce hepatocytes and maintain ectopic protein production in them for several weeks. Accordingly, DNASE1L3 activity in the sera of Ad-DNASE1L3-treated KO mice was restored at 4 weeks, but largely disappeared at 12 weeks post-injection (Figure 3H). Importantly, the development of anti-dsDNA IgG titers was transiently but significantly delayed in KO animals treated with Ad-DNASE1L3 compared to the control Ad-GFP (Figure 3I). Collectively, these results show that circulating DNASE1L3 restricts anti-DNA autoreactivity, likely targeting an extracellular DNA substrate.

Circulating DNASE1L3 Is Produced by Mononuclear Phagocytes

We explored the hematopoietic cell type responsible for the production of circulating DNASE1L3. Microarray expression datasets suggested a restricted expression of *DNASE1L3* in dendritic cells (DC) in both humans and mice (Figures S4A and S4B), as confirmed by qRT-PCR (Figure S4C). In addition, the expression of *Dnase1l3* was apparent in macrophages (MΦ) in select tissues, including the spleen, liver, and intestine (Figure S4B). We used the fluorescent detection of LacZ in the targeted *Dnase1l3* allele to confirm the highest expression of *Dnase1l3* in conventional DC (cDC) and in a small fraction of splenic MΦ (Figure 4A). Consistent with microarray and qRT-PCR data (Figures S4B and S4C), low levels of expression were also detected in plasmacy-toid DC (pDC), MZB, and B-1a cells (Figure 4A).

Lymphocyte-deficient *Rag1*$^{-/-}$ mice had normal levels of serum DNASE1L3, ruling out the contribution of B cells (Figure 4B). In contrast, a transient depletion of CD11c^{hi} cells (which include all cDC and intestinal MΦ) reduced serum DNASE1L3 by >75% (Figure 4C). Treatment of WT mice with clodronate liposomes (which deplete tissue MΦ as well as reduce cDC numbers; Figure S4D) reduced serum DNASE1L3 by ~50% (Figure 4D). Finally, a single treatment with anti-Csf1r Ab (which primarily depletes intestinal MΦ) reduced serum DNASE1L3 by ~15% (Figure 4E). Because tissue MΦ are slowly replaced after BM transfer (Lavin et al., 2015), the production of DNASE1L3 by MΦ may explain the relatively slow decline of DNASE1L3 levels in KO → WT chimeras (Figure 3F). We conclude that circulating DNASE1L3 is predominantly produced by mononuclear phagocytes, including cDC and certain tissue MΦ.

DNASE1L3 Digests Chromatin in Apoptotic Cell-Derived Microparticles

To identify the putative extracellular DNA substrate of DNASE1L3, we examined the ability of recombinant human DNASE1L3 to digest different forms of DNA. As reported previously (Wilber et al., 2002) and confirmed by the analysis of KO mice (Figure 3E), DNASE1L3, but not DNASE1, could digest liposome-coated plasmid DNA (Figures 5A and 5B). In addition, DNASE1L3 was more efficient than DNASE1 in digesting genomic DNA within native polynucleosomes (Figure 5C). The polymorphic R206C variant of DNASE1L3

Author Manuscript Author Manuscript Author Manuscript Author Manuscript

showed a reduced enzymatic activity on all DNA substrates (Figures 5B and 5C). In contrast, both specific activities of DNASE1L3, but not the digestion of “naked” DNA, were abolished by the deletion of its C-terminal peptide (Figures 5B and 5C). Molecular modeling of DNASE1L3 by homology to DNASE1 suggested that the C-terminal peptide comprises a stable α-helix protruding at a fixed angle from the conserved DNase domain (Figures S5A–S5E). Its stable helical conformation and the positive charge likely facilitate both the membrane binding/penetration and the displacement of DNA from bound histones.

Microparticles (MP) released from apoptotic cells are akin to liposomes and contain nucleosomal DNA (Pisetsky et al., 2011). Indeed, DNASE1L3, but not DNASE1, digested genomic DNA in MP generated from apoptotic Jurkat T cells (Figure 5D) and primary splenocytes (data not shown). MP showed low propidium iodide staining unless permeabilized (data not shown), suggesting that DNASE1L3 can penetrate intact MP membranes. Similar to the digestion of liposome-coated and polynucleosomal DNA, the digestion of MP DNA was slightly reduced by the R206C polymorphism, but completely abolished by the C-terminal deletion. As previously reported (Ullal et al., 2011), a fraction of MP can be stained with anti-DNA/histone 2a/2b monoclonal Ab (mAb) PR1-3 (Figure 5E). The staining was enhanced by fixation/permeabilization (data not shown), confirming that MP contain chromatin both internally and at the surface. The PR1-3 staining was abolished by pre-treatment with DNASE1L3, but not by the C-terminal deletion mutant of DNASE1L3 or by DNASE1 (Figure 5E).

We examined DNASE1L3 variants with a hexahistidine (His) tag near the C-terminal peptide (Figure 5A). The tag at the C terminus (His-CT) abolished the digestion of both liposome-coated and nucleosomal DNA, whereas the tag preceding the C-terminal peptide (His-preCT) abolished only the digestion of nucleosomal DNA (Figure 5F). The His-preCT tag is predicted to change the conformation of the C-terminal α-helical peptide relative to the DNase domain (Figure S5E). Importantly, this tag prevented the digestion of DNA within MP (Figure 5F) and on their surface (Figure 5G), suggesting that the ability to digest nucleosomal DNA is essential for this activity.

Consistent with in vitro results, serum from KO animals was unable to digest liposome-coated DNA even after prolonged incubation (Figure 5H). It was also unable to digest polynucleosomes during a short (15-min) incubation (Figure 5I), although longer incubation resulted in complete digestion (Figure S5F). Importantly, the serum from KO animals was completely unable to digest MP DNA (Figure 5J). Thus, DNASE1L3 has two unique and separable activities, i.e., the digestion of liposome-coated DNA and of nucleosomal DNA. These activities enable DNASE1L3 to digest chromatin within and on the surface of apoptotic MP, suggesting this DNA forms as a natural substrate of DNASE1L3.

DNASE1L3 Restricts the Amount of DNA in Circulating Microparticles

We tested the relationship between DNASE1L3 and the DNA content of MP in vivo. Following intravenous (i.v.) injection of Jurkat cell MP, their DNA was rapidly cleared from WT mice, but persisted in the serum, spleen, and liver of KO mice (Figure S6A). We then analyzed endogenous MP from murine plasma, characterized by their small size, the absence of platelet and erythrocyte markers, and positivity for apoptotic cell marker Annexin V

Author Manuscript Author Manuscript Author Manuscript Author Manuscript

(Figure S6B). Although the number of MP in the plasma of KO mice was unchanged (Figure S6C), their genomic DNA content was increased >100-fold (Figure 6A). Accordingly, the amount of DNA in total plasma from KO mice was increased >10-fold (Figure 6B). Furthermore, a fraction of plasma MP from young KO animals exposed chromatin on their surface, as revealed by positive staining with PR1-3 (Figure 6C).

To test whether DNASE1L3 similarly digests circulating MP DNA in humans, we analyzed two DNASE1L3 null patients with HUVS (Ozçakar et al., 2013). Neither patient 1 (HUVS +SLE in remission) nor patient 2 (HUVS only) had active SLE, ruling out any secondary effects of the disease. Using the digestion of liposome-coated plasmid DNA, we confirmed that the patients had no DNASE1L3 activity in plasma, whereas their haplodeficient parents showed ~50% activity (Figure 6D). We also analyzed three additional subjects who were heterozygous for the R206C variant of DNASE1L3. These subjects manifested ~60% of control DNASE1L3 activity in plasma (Figure 6D), suggesting that the R206C variant is ~5-fold less active than the common variant.

Plasma of DNASE1L3 null patients failed to digest nucleosomal DNA (Figure 6E), as well as MP DNA (Figure 6F), and even the plasma of haplodeficient parents showed detectable impairments in these assays. We then isolated endogenous plasma MP from the human plasma and confirmed that Annexin V^+ MP express markers of leukocytes and include a granulocyte marker-positive fraction (Figure S6D) (Nielsen et al., 2011). MP from DNASE1L3 null patients contained >1,000-fold more DNA than those from healthy controls, and MP from haplodeficient parents or R206C carriers also showed an increased DNA content (Figure 6G). The analysis of human plasma samples showed that nearly all detectable genomic DNA is contained within the MP fraction (Figure S6E). Accordingly, total unfractionated plasma of DNASE1L3 null patients also harbored increased amounts of circulating DNA (Figure 6H). Collectively, genetic evidence in animals and humans demonstrates that DNASE1L3 digests genomic DNA circulating in plasma, specifically within apoptotic cell-derived MP.

DNASE1L3 Prevents the Recognition of Microparticle DNA by Auto-Abs

We tested whether the DNASE1L3-sensitive chromatin on the surface of microparticles is targeted by auto-Abs in experimental SLE. The serum of KO mice from a young age contained IgG binding to Jurkat MP (Figures 7A and 7B). The binding was abolished by pre-treatment of MP with DNASE1L3 (Figure 7C), confirming that it is directed toward DNASE1L3-sensitive chromatin on their surface. Similar DNASE1L3-sensitive binding was also displayed by several anti-DNA/anti-nucleosome mAbs from mouse SLE models (Figure S7A), including the prototypic mAb 3H9 (Shlomchik et al., 1987). To directly test whether MP can elicit anti-DNA responses, we injected wild-type animals with MP generated from syngeneic apoptotic splenocytes. MP injections in animals treated with the IFN adenovirus, but not in naive animals, induced high titers of anti-nucleosome IgG (Figure 7D). Thus, in the context of elevated IFN, MP can represent antigens that elicit chromatin-specific B cell responses.

We asked whether DNASE1L3-sensitive chromatin in MP is recognized by auto-Abs in human SLE. The *DNASE1L3*-deficient patient 1 (HUVS+SLE in remission), but not patient

Author Manuscript Author Manuscript Author Manuscript Author Manuscript

2 (HUVS without SLE), or their healthy parents harbored serum IgG binding to MP in a DNASE1L3-sensitive manner (Figure 7E). Human IgG carrying the 9G4 idiotope are prominent among SLE-associated auto-Abs and bind multiple antigens, including DNA, cell nuclei, and apoptotic cell membranes (Jenks et al., 2013; Richardson et al., 2013). Two $9G4^+$ mAb clones from SLE patients (75G15 and 74C2) that show strong binding to apoptotic cell membranes (Richardson et al., 2013) showed DNASE1L3-sensitive binding to MP(Figure S7B). Finally, we tested whether DNASE1L3-sensitive chromatin on MP represents an antigen in patients with sporadic SLE. None of healthy control subjects (n = 10) and 64% of SLE patients (n = 53) harbored IgG binding to MP (Figures S7C, S7F, and S7G). The binding to MP showed a weak but significant correlation with anti-dsDNA titers (data not shown), as observed for IgG binding to endogenous MP in SLE (Ullal et al., 2011). Importantly, the binding was sensitive to DNASE1L3 pre-treatment in ~36% of patients (Figures S7C, S7F, and S7G), suggesting that it is directed against chromatin components on the surface of MP. Collectively, our data in mice and humans suggest that chromatin on circulating apoptotic MP is an antigen for DNA-reactive B cells and Abs produced by them. This chromatin is a physiological substrate for circulating DNASE1L3, which limits its availability and may thereby protect from anti-DNA reactivity and SLE.

DISCUSSION

SLE in *DNASE1L3*-deficient human patients is characterized by early onset, absence of a sex bias, and the presence of anti-dsDNA IgG (Al-Mayouf et al., 2011; Ozçakar et al., 2013). These features were recapitulated in *Dnase1l3*-deficient mice, all of which develop anti-dsDNA reactivity on two distinct genetic backgrounds. Hereditary SLE has been difficult to model in mice: for instance, null mutations in the complement component *C1Q* cause SLE in human patients (Ghodke-Puranik and Niewold, 2015; Picard et al., 2015), but no overt pathology in mice (Heidari et al., 2006). Thus, our results establish a mouse model of familial SLE and confirm DNASE1L3 as an evolutionarily conserved mediator of tolerance to DNA.

Dnase1l3-deficient mice rapidly developed IgG to dsDNA and particularly to chromatin, whereas the reactivity to other self-antigens was either absent or developed later. Similarly, major signs of immune activation (splenomegaly, GC reaction, and T cell activation) appeared only in old animals. This delay likely reflects the lack of additional disease-promoting mutations common in SLE models, such as those causing lymphoproliferation (e.g., Fas^{lpr}) or heightened RNA sensing (e.g., *Yaa*). Another important aspect is the paucity of immune stimulation in specific pathogen-free mice as opposed to human patients. Indeed, the treatment with IFN induced anti-RNA response, accelerated immune activation, and caused significant mortality. These data suggest that the reactivity to nucleosomal DNA within chromatin causes all subsequent pathological features and can yield a severe SLE-like disease following an inflammatory stimulus.

Ablation of STING-dependent cytoplasmic DNA sensing abolishes inflammatory disease caused by DNASE2 or TREX1 deficiency (Ahn et al., 2012; Gall et al., 2012), but exacerbates autoimmunity in polygenic or chemically induced models (Sharma et al., 2015). In contrast, the deletion of STING had a minimal effect on anti-DNA responses or the

Author Manuscript Author Manuscript Author Manuscript Author Manuscript

ensuing disease in *Dnase1l3*-deficient mice. The observed essential role of MyD88 may reflect its activity downstream of TLRs or IL-1 receptor; the specific signal(s) involved remain to be identified but are likely to be cell extrinsic. Notably, no signs of activation or developmental abnormalities could be detected in DCs or B cells from young *Dnase1l3* null mice. Therefore, the primary anti-DNA Ab response may result from direct antigen receptor-mediated expansion and plasmablast differentiation of DNA-reactive B cells, likely via extrafollicular activation and class switching. These antigen-specific primary signals may be further amplified by MyD88-dependent signals in B cells and/or other cell types. Collectively, the mechanism of anti-DNA reactivity in *Dnase1l3*-deficient mice likely reflects the primary loss of antigen-specific B cell tolerance to DNA.

The development of anti-dsDNA Abs inversely correlated with the levels of circulating DNASE1L3, suggesting that DNASE1L3 acts in a cell-extrinsic manner to shield autoreactive B cells from antigenic self-DNA. Notably, we found that *Dnase1l3* is expressed in DCs and select tissue macrophages, which produce the bulk of secreted DNASE1L3. These observations support the role of DCs and macrophages in self-tolerance and restriction of autoimmunity (Ganguly et al., 2013; Lavin et al., 2015). This tolerogenic function has been primarily associated with engulfment of apoptotic cells, induction of T cell tolerance, and expression of anti-inflammatory cytokines and surface molecules by the phagocytes. Our work describes a different mechanism of tolerogenic activity by these cells, whereby their secretion of a DNA-processing enzyme enforces global B cell tolerance to DNA.

Our data show that DNASE1L3 (1) systemically acts in a cell-extrinsic manner, (2) has a unique capacity to digest membrane-encapsulated DNA, and (3) has a preferential capacity to digest DNA within nucleosomes. These properties point to the chromatin within circulating MP as the physiological substrate of DNASE1L3. DNA-containing MP are normally present in the human plasma (Dieker et al., 2016; Nielsen et al., 2011, 2012) and are derived from cells that die within the vessel lumen, such as rapidly turning over myeloid cells. Notably, the majority of genomic DNA detectable in human plasma was contained within the MP fraction. Indeed, total human plasma DNA was shown to be primarily derived from leukocytes and to comprise nucleosomal fragments of chromatin (Holdenrieder et al., 2005; Snyder et al., 2016; Sun et al., 2015). Accordingly, DNASE1L3 deficiency increased both the DNA cargo of circulating MP and the total amount of DNA in the plasma of *DNASE1L3*-deficient animals and human subjects. Although other potential DNA substrates of DNASE1L3 cannot be ruled out, these data implicate micro-particle-associated DNA as the relevant endogenous target of DNASE1L3.

Chromatin in apoptotic blebs and circulating MP becomes exposed at the membrane surface and accessible to auto-Abs (Casciola-Rosen et al., 1994; Radic et al., 2004; Ullal et al., 2011). This chromatin would be accessible to DNA-reactive B cells, comprising a potentially antigenic form of DNA. We found that exposed chromatin on MP is digested by DNASE1L3 and becomes a target of auto-Abs in *Dnase1l3*-deficient animals and in the *DNASE1L3*-deficient human patient with SLE history. Importantly, DNASE1L3-sensitive chromatin on the surface of MP appears to be targeted by prototypic autoreactive clones from murine and human SLE, as well as by serum IgG from at least one-third of patients

Author Manuscript Author Manuscript Author Manuscript Author Manuscript

with sporadic SLE. The latter is consistent with the binding of IgG and complement to plasma MP in human SLE patients (Nielsen et al., 2012; Ullal et al., 2011). Therefore, micro-particle-associated chromatin appears to represent a common antigenic form of self-DNA in SLE.

In conclusion, we identify chromatin in microparticles as a latent self-antigen for autoreactive B cells and circulating DNASE1L3 as an essential factor that restricts chromatin antigenicity and prevents anti-DNA responses. These results provide a mechanistic explanation for the association of null and hypomorphic DNASE1L3 mutations with familial and sporadic SLE, respectively. They also uncover a cell-extrinsic mechanism of tolerance to DNA that involves a secreted enzyme and therefore can be developed for therapeutic purposes. In particular, the observed delay of anti-DNA reactivity by DNASE1L3 re-expression warrants the exploration of DNASE1L3 protein delivery as a therapeutic tool in SLE and other systemic autoimmune diseases.

EXPERIMENTAL PROCEDURES

Animals

All experiments were performed according to the investigator's protocol approved by the Institutional Animal Care and Use Committees of Columbia University and New York University. Mice with a targeted germline replacement of *Dnase1l3* (*Dnase1l3*^{LacZ}) were purchased from Taconic Knockout Repository (model TF2732), backcrossed onto 129SvEvTac or C57BL/6 backgrounds for >10 generations, and intercrossed to obtain *Dnase1l3*$^{LacZ/LacZ}$ knockout animals. Age-matched wild-type mice of the respective backgrounds were bred in the same animal colony and used as controls. Genetic deletion of STING and MyD88, hematopoietic reconstitution, and cell-depletion experiments are described in the Supplemental Experimental Procedures.

Human Subjects

DNASE1L3-deficient HUVS patients 1 and 2 correspond to patients IV-4 and IV-5 from family 1 described in (Ozçakar et al., 2013). Their study was approved by the Ethics Committees of Ankara University (Turkey) and the IRB at the University of Miami, and informed consents were obtained from the parents. Blood from patients with sporadic SLE and healthy controls was obtained from the NYU IRB-approved Rheumatology SAMPLE (Specimen and Matched Phenotype Linked Evaluation) Biorepository. All patients signed an IRB-approved informed consent. Additional information is provided in the Supplemental Experimental Procedures.

Adenoviruses

Adenoviral vector encoding IFN-α5 has been previously described (Mathian et al., 2005). Adenoviral vector-encoding human DNASE1L3 was constructed by Welgen. Adenoviral particles were produced and purified at Welgen and were injected into the indicated mice i.v. at 0.5 to 1 × 10^{10} particles per mouse.

Author Manuscript Author Manuscript Author Manuscript Author Manuscript

Analysis of Autoreactivity

Flow cytometry, immunochemistry, ANA, ELISA, ELISPOT, antigen arrays, and the analysis of kidney IgG deposition and histopathology are described in the Supplemental Experimental Procedures.

Recombinant DNases

Cloned open reading frame (ORF) of human DNASE1 and DNASE1L3 (NCBI: NP_004935.1) were subcloned into pMCSV-IRES-GFP (pMIG) retroviral expression vector. The constructs for DNASE1L3 variants were generated using the Q5 site-directed mutagenesis kit (NEB) and included the R206 → C substitution, the C-terminal truncation (amino acids [aa] 282–305), and the insertions of hexahistidine between aa 282–283 (His-preCT) or between aa 305 and the stop codon (His-CT). The resultant constructs or the empty pMIG were used as plasmids for the transient transfection of HEK293 cells, with equal efficiency of transfection confirmed by GFP expression. To avoid contamination with DNases in bovine serum, transfection was performed in medium with 15% KnockOUT serum supplement (Thermo Fisher). Transfected cells were cultured for 48 hr, and the supernatants were collected, filtered, supplemented with 4 mM $CaCl_2$ and 4 mM $MgCl_2$, and frozen in aliquots.

Analysis of DNASE1L3 Activity

To measure the digestion of liposome-coated DNA, pMIG plasmid DNA was pre-incubated with DOTAP (Roche) in HBSS. Native or DOTAP-coated plasmid (1 ng/reaction) was incubated with an equal volume of DNase-containing supernatants or sera for 60 min at 37°C in a total volume of 2 μl. The amount of remaining DNA was measured by qPCR with GFP-specific primers and expressed as a percent of input DNA using a calibration curve with serial plasmid dilutions. For the measurement of relative DNASE1L3 activity in vivo, the digestion was performed for 10 min using 1 μl of mouse serum or human serum or plasma in a final volume of 5 μl. After qPCR, the amount of remaining DNA was converted to a percent of DNASE1L3 activity using a calibration curve with serial dilutions of control wild-type serum or plasma.

Purified human polynucleosomes from HeLa cells (Epicypher) or purified Jurkat cell DNA (2 ng/reaction) were incubated with an equal volume of DNase-containing supernatants for 15 min at 37°C in a total volume of 2 μl. The amount of remaining DNA was measured by qPCR with primers specific for human genomic *Alu* repeats and expressed as a percent of input DNA using a calibration curve with serial DNA dilutions.

Generation and Analysis of Microparticles

MP from Jurkat cells were generated as previously described (Ullal et al., 2011). Briefly, the cells were cultured in the presence of 1 mM staurosporine (Sigma-Aldrich) overnight, harvested, and collected by centrifugation for 5 min at 1,500 rpm. The supernatants were collected and centrifuged at 22,000 × *g* for 30 min to pellet the MP, which were analyzed on the Accuri C6 flow cytometer (BD Biosciences) to determine absolute numbers and ensure >95% enrichment. Where indicated, MP (10^5/μl in PBS) were incubated with an equal volume of DNase-containing transfection supernatants for 1 hr at 37°C. The generation and

Author Manuscript Author Manuscript Author Manuscript Author Manuscript

administration of MP from mouse splenocytes is described in the Supplemental Experimental Procedures.

To isolate MP from human plasma, blood was collected in tubes containing EDTA, and blood cells were removed by centrifugation at 2,000 × *g* for 10 min at 4°C. In some experiments, a second centrifugation step (3,000 × *g* for 10 min) was used to remove platelets as previously described (Nielsen et al., 2011). The resultant plasma (either fresh or stored at −80°C) was centrifuged at 22,000 × *g* for 30–60 min to pellet the MP, and the supernatant was used to measure DNASE1L3 activity and Ab binding specificities. To isolate MP from murine plasma, animals were euthanized and immediately exsanguinated by cardiac puncture into heparin-containing tubes. Plasma was isolated by centrifugation at 2,000 × *g* for 10 min 4°C and centrifuged at 22,000 × *g* for 30 min to pellet the MP. Plasma MP were resuspended and counted by flow cytometry after staining for CD42b and CD235a (human) or CD41 and Ter119 (mouse) to exclude platelets and erythrocytes.

To test the ability of mouse serum or human plasma to digest MP DNA, Jurkat MP (5×10^5/μl in PBS) were incubated with an equal volume of serum/plasma for 1 hr at 37°C in a final reaction volume of 10 μl. The DNA content of Jurkat cell-derived MP, human plasma MP, and total plasma was measured by qPCR for human genomic *Alu* repeats. The DNA content of murine plasma MP and total plasma was measured by qPCR for mouse genomic *B1* repeats. Data were converted into the amount of genomic DNA using calibration curves with the respective genomic DNA and expressed as the percent of input DNA or as amount of DNA per MP.

For surface staining, 2.5×10^5 native or DNase-treated Jurkat cell MP were stained with either purified anti-DNA/histone 2a/2b mAb PR1-3 (10 μg/ml) or mouse sera (1:10 dilution) for 30 min at 4°C. Stained MP were washed by centrifugation at 22,000 × *g* for 30 min, incubated with PE-labeled goat anti–mouse IgG secondary Ab (eBioscience) at a 1:200 dilution for 30 min at 4°C, and analyzed by flow cytometry without further washing. Staining with human sera or plasma was done as above at 1:20 dilution, using PE-labeled goat anti-human IgG secondary Ab (eBioscience).

Statistics

Statistical significance was estimated by nonparametric Mann-Whitney test.

Supplementary Material

Refer to Web version on PubMed Central for supplementary material.

Acknowledgments

We thank G. Silverman for help and discussions, M. Shlomchik and A. Davidson for reagents, and S. Rasmussen for technical assistance. This work was supported by NIH grants (AR064460 and AI072571 to B.R.; DK098378 to I.I.I.), the Lupus Research Institute (to B.R.), the Judith and Stewart Colton Center for Autoimmunity (to B.R. and J.P.B.), and the Irvington Institute Fellowship of the Cancer Research Institute (to V.S.). K.B.E. is a co-founder and consultant of Resolve Therapeutics, which develops soluble nucleases for therapeutic purposes.

Author Manuscript Author Manuscript Author Manuscript Author Manuscript

References

Ahn J, Gutman D, Saijo S, Barber GN. STING manifests self DNA-dependent inflammatory disease. Proc Natl Acad Sci USA. 2012; 109:19386–19391. [PubMed: 23132945]

Al-Mayouf SM, Sunker A, Abdwani R, Abrawi SA, Almurshedi F, Alhashmi N, Al Sonbul A, Sewairi W, Qari A, Abdallah E, et al. Loss-of-function variant in DNASE1L3 causes a familial form of systemic lupus erythematosus. Nat Genet. 2011; 43:1186–1188. [PubMed: 22019780]

Baron WF, Pan CQ, Spencer SA, Ryan AM, Lazarus RA, Baker KP. Cloning and characterization of an actin-resistant DNase I-like endonuclease secreted by macrophages. Gene. 1998; 215:291–301. [PubMed: 9714828]

Caielli S, Athale S, Domic B, Murat E, Chandra M, Banchereau R, Baisch J, Phelps K, Clayton S, Gong M, et al. Oxidized mitochondrial nucleoids released by neutrophils drive type I interferon production in human lupus. J Exp Med. 2016; 213:697–713. [PubMed: 27091841]

Casciola-Rosen LA, Anhalt G, Rosen A. Autoantigens targeted in systemic lupus erythematosus are clustered in two populations of surface structures on apoptotic keratinocytes. J Exp Med. 1994; 179:1317–1330. [PubMed: 7511686]

Choi J, Kim ST, Craft J. The pathogenesis of systemic lupus erythematosus-an update. Curr Opin Immunol. 2012; 24:651–657. [PubMed: 23131610]

Crow YJ. Type I interferonopathies: mendelian type I interferon up-regulation. Curr Opin Immunol. 2015; 32:7–12. [PubMed: 25463593]

Dieker J, Tel J, Pieterse E, Thielen A, Rother N, Bakker M, Fransen J, Dijkman HB, Berden JH, de Vries JM, et al. Circulating apoptotic microparticles in systemic lupus erythematosus patients drive the activation of dendritic cell subsets and prime neutrophils for NETosis. Arthritis Rheumatol. 2016; 68:462–472. [PubMed: 26360137]

Ehlers M, Fukuyama H, McGaha TL, Aderem A, Ravetch JV. TLR9/MyD88 signaling is required for class switching to pathogenic IgG2a and 2b autoantibodies in SLE. J Exp Med. 2006; 203:553–561. [PubMed: 16492804]

Gall A, Treuting P, Elkon KB, Loo YM, Gale M Jr, Barber GN, Stetson DB. Autoimmunity initiates in nonhematopoietic cells and progresses via lymphocytes in an interferon-dependent autoimmune disease. Immunity. 2012; 36:120–131. [PubMed: 22284419]

Ganguly D, Haak S, Sisirak V, Reizis B. The role of dendritic cells in autoimmunity. Nat Rev Immunol. 2013; 13:566–577. [PubMed: 23827956]

Ghodke-Puranik Y, Niewold TB. Immunogenetics of systemic lupus erythematosus: A comprehensive review. J Autoimmun. 2015; 64:125–136. [PubMed: 26324017]

Heidari Y, Bygrave AE, Rigby RJ, Rose KL, Walport MJ, Cook HT, Vyse TJ, Botto M. Identification of chromosome intervals from 129 and C57BL/6 mouse strains linked to the development of systemic lupus erythematosus. Genes Immun. 2006; 7:592–599. [PubMed: 16943797]

Holdenrieder S, Stieber P, Chan LY, Geiger S, Kremer A, Nagel D, Lo YM. Cell-free DNA in serum and plasma: comparison of ELISA and quantitative PCR. Clin Chem. 2005; 51:1544–1546. [PubMed: 16040855]

Jenks SA, Palmer EM, Marin EY, Hartson L, Chida AS, Richardson C, Sanz I. 9G4+ autoantibodies are an important source of apoptotic cell reactivity associated with high levels of disease activity in systemic lupus erythematosus. Arthritis Rheum. 2013; 65:3165–3175. [PubMed: 23983101]

Lavin Y, Mortha A, Rahman A, Merad M. Regulation of macrophage development and function in peripheral tissues. Nat Rev Immunol. 2015; 15:731–744. [PubMed: 26603899]

Lood C, Blanco LP, Purmalek MM, Carmona-Rivera C, De Ravin SS, Smith CK, Malech HL, Ledbetter JA, Elkon KB, Kaplan MJ. Neutrophil extracellular traps enriched in oxidized mitochondrial DNA are interferogenic and contribute to lupus-like disease. Nat Med. 2016; 22:146–153. [PubMed: 26779811]

Martin JE, Assassi S, Diaz-Gallo LM, Broen JC, Simeon CP, Castellvi I, Vicente-Rabaneda E, Fonollosa V, Ortego-Centeno N, González-Gay MA, et al. Spanish Scleroderma Group; SLEGEN consortium; USScleroderma GWAS group; BIOLUPUS. A systemic sclerosis and systemic lupus erythematosus pan-meta-GWAS reveals new shared susceptibility loci. Hum Mol Genet. 2013; 22:4021–4029. [PubMed: 23740937]

Author Manuscript Author Manuscript Author Manuscript Author Manuscript

Mathian A, Weinberg A, Gallegos M, Banchereau J, Koutouzov S. IFN-alpha induces early lethal lupus in preautoimmune (New Zealand Black x New Zealand White) F1 but not in BALB/c mice. J Immunol. 2005; 174:2499–2506. [PubMed: 15728455]

Mayes MD, Bossini-Castillo L, Gorlova O, Martin JE, Zhou X, Chen WV, Assassi S, Ying J, Tan FK, Arnett FC, et al. Spanish Scleroderma Group. Immunochip analysis identifies multiple susceptibility loci for systemic sclerosis. Am J Hum Genet. 2014; 94:47–61. [PubMed: 24387989]

Mizuta R, Araki S, Furukawa M, Furukawa Y, Ebara S, Shiokawa D, Hayashi K, Tanuma S, Kitamura D. DNase γ is the effector endonuclease for internucleosomal DNA fragmentation in necrosis. PLoS ONE. 2013; 8:e80223. [PubMed: 24312463]

Nagata S, Kawane K. Autoinflammation by endogenous DNA. Adv Immunol. 2011; 110:139–161. [PubMed: 21762818]

Napirei M, Wulf S, Eulitz D, Mannherz HG, Kloeckl T. Comparative characterization of rat deoxyribonuclease 1 (Dnase1) and murine deoxyribonuclease 1-like 3 (Dnase1l3). Biochem J. 2005; 389:355–364. [PubMed: 15796714]

Napirei M, Ludwig S, Mezrhab J, Klöckl T, Mannherz HG. Murine serum nucleases–contrasting effects of plasmin and heparin on the activities of DNase1 and DNase1-like 3 (DNase1l3). FEBS J. 2009; 276:1059–1073. [PubMed: 19154352]

Nielsen CT, Østergaard O, Johnsen C, Jacobsen S, Heegaard NH. Distinct features of circulating microparticles and their relationship to clinical manifestations in systemic lupus erythematosus. Arthritis Rheum. 2011; 63:3067–3077. [PubMed: 21702008]

Nielsen CT, Østergaard O, Stener L, Iversen LV, Truedsson L, Gullstrand B, Jacobsen S, Heegaard NH. Increased IgG on cell-derived plasma microparticles in systemic lupus erythematosus is associated with autoantibodies and complement activation. Arthritis Rheum. 2012; 64:1227–1236. [PubMed: 22238051]

Ozçakar ZB, Foster J 2nd, Diaz-Horta O, Kasapcopur O, Fan YS, Yalçınkaya F, Tekin M. DNASE1L3 mutations in hypocomplementemic urticarial vasculitis syndrome. Arthritis Rheum. 2013; 65:2183–2189. [PubMed: 23666765]

Picard C, Mathieu AL, Hasan U, Henry T, Jamilloux Y, Walzer T, Belot A. Inherited anomalies of innate immune receptors in pediatric-onset inflammatory diseases. Autoimmun Rev. 2015; 14:1147–1153. [PubMed: 26269221]

Pisetsky DS. Anti-DNA antibodies - quintessential biomarkers of SLE. Nat Rev Rheumatol. 2016; 12:102–110. [PubMed: 26581343]

Pisetsky DS, Gauley J, Ullal AJ. Microparticles as a source of extracellular DNA. Immunol Res. 2011; 49:227–234. [PubMed: 21132466]

Radic M, Marion T, Monestier M. Nucleosomes are exposed at the cell surface in apoptosis. J Immunol. 2004; 172:6692–6700. [PubMed: 15153485]

Rekvig OP, van der Vlag J, Seredkina N. Review: antinucleosome antibodies: a critical reflection on their specificities and diagnostic impact. Arthritis Rheumatol. 2014; 66:1061–1069. [PubMed: 24470458]

Richardson C, Chida AS, Adlowitz D, Silver L, Fox E, Jenks SA, Palmer E, Wang Y, Heimburg-Molinaro J, Li QZ, et al. Molecular basis of 9G4 B cell autoreactivity in human systemic lupus erythematosus. J Immunol. 2013; 191:4926–4939. [PubMed: 24108696]

Santiago-Raber ML, Amano H, Amano E, Baudino L, Otani M, Lin Q, Nimmerjahn F, Verbeek JS, Ravetch JV, Takasaki Y, et al. Fcgamma receptor-dependent expansion of a hyperactive monocyte subset in lupus-prone mice. Arthritis Rheum. 2009; 60:2408–2417. [PubMed: 19644866]

Sharma S, Campbell AM, Chan J, Schattgen SA, Orlowski GM, Nayar R, Huyler AH, Nündel K, Mohan C, Berg LJ, et al. Suppression of systemic autoimmunity by the innate immune adaptor STING. Proc Natl Acad Sci USA. 2015; 112:E710–E717. [PubMed: 25646421]

Shlomchik MJ, Aucoin AH, Pisetsky DS, Weigert MG. Structure and function of anti-DNA autoantibodies derived from a single autoimmune mouse. Proc Natl Acad Sci USA. 1987; 84:9150–9154. [PubMed: 3480535]

Snyder MW, Kircher M, Hill AJ, Daza RM, Shendure J. Cell-free DNA comprises an in vivo nucleosome footprint that informs its tissues-of-origin. Cell. 2016; 164:57–68. [PubMed: 26771485]

Author Manuscript Author Manuscript Author Manuscript Author Manuscript

Sun K, Jiang P, Chan KC, Wong J, Cheng YK, Liang RH, Chan WK, Ma ES, Chan SL, Cheng SH, et al. Plasma DNA tissue mapping by genome-wide methylation sequencing for noninvasive prenatal, cancer, and transplantation assessments. Proc Natl Acad Sci USA. 2015; 112:E5503–E5512. [PubMed: 26392541]

Ueki M, Takeshita H, Fujihara J, Iida R, Yuasa I, Kato H, Panduro A, Nakajima T, Kominato Y, Yasuda T. Caucasian-specific allele in non-synonymous single nucleotide polymorphisms of the gene encoding deoxyribonuclease I-like 3, potentially relevant to autoimmunity, produces an inactive enzyme. Clin Chim Acta. 2009; 407:20–24. [PubMed: 19559017]

Ullal AJ, Reich CF 3rd, Clowse M, Criscione-Schreiber LG, Tochacek M, Monestier M, Pisetsky DS. Microparticles as antigenic targets of antibodies to DNA and nucleosomes in systemic lupus erythematosus. J Autoimmun. 2011; 36:173–180. [PubMed: 21376534]

Ullal AJ, Marion TN, Pisetsky DS. The role of antigen specificity in the binding of murine monoclonal anti-DNA antibodies to microparticles from apoptotic cells. Clin Immunol. 2014; 154:178–187. [PubMed: 24873886]

Volkman HE, Stetson DB. The enemy within: endogenous retroelements and autoimmune disease. Nat Immunol. 2014; 15:415–422. [PubMed: 24747712]

Wardemann H, Nussenzweig MC. B-cell self-tolerance in humans. Adv Immunol. 2007; 95:83–110. [PubMed: 17869611]

Wilber A, Lu M, Schneider MC. Deoxyribonuclease I-like III is an inducible macrophage barrier to liposomal transfection. Mol Ther. 2002; 6:35–42. [PubMed: 12095301]

Zochling J, Newell F, Charlesworth JC, Leo P, Stankovich J, Cortes A, Zhou Y, Stevens W, Sahhar J, Roddy J, et al. An Immunochip-based interrogation of scleroderma susceptibility variants identifies a novel association at DNASE1L3. Arthritis Res Ther. 2014; 16:438. [PubMed: 25332064]

Author Manuscript Author Manuscript Author Manuscript Author Manuscript

Highlights

- Rapid anti-DNA antibody response, followed by SLE in *Dnase1l3*-deficient mice
- Autoreactivity is repressed by circulating DNASE1L3 and is independent of STING
- DNASE1L3 digests genomic DNA in microparticles released from apoptotic cells
- DNASE1L3 prevents autoantibody binding to chromatin on microparticle surface

Author Manuscript Author Manuscript Author Manuscript Author Manuscript

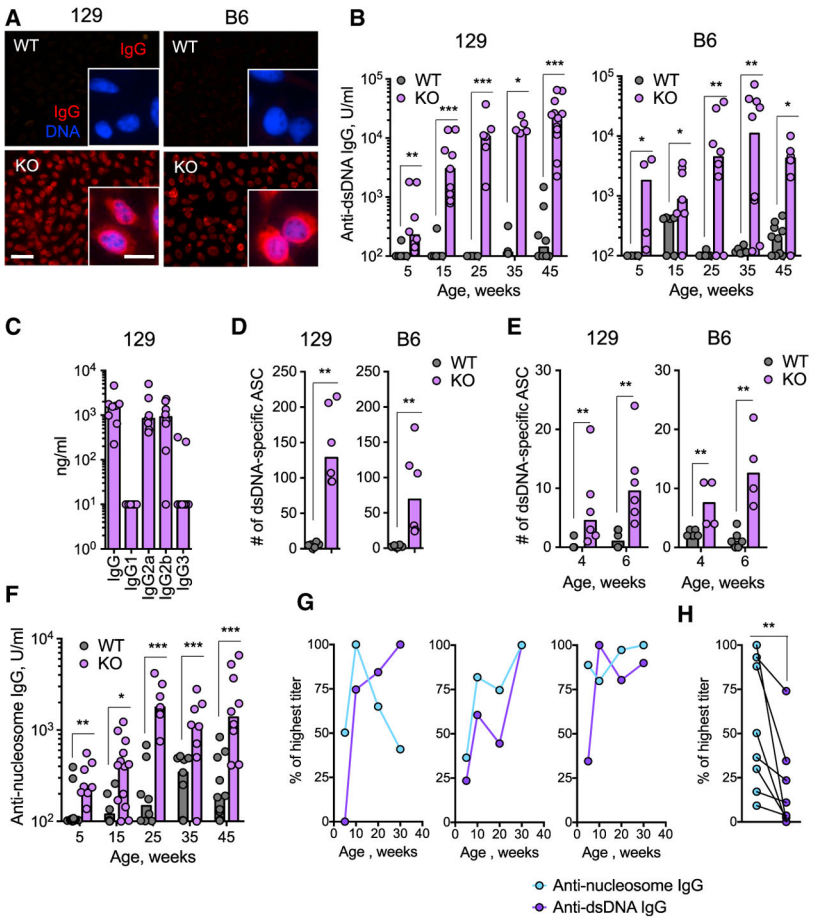

Figure 1. *Dnase1l3*-Deficient Mice Develop Abs to dsDNA and Chromatin

(A) ANA in the sera of *Dnase1l3* knockout (KO) and control wild-type (WT) mice. Fixed Hep2 cells incubated with sera from 50-week-old mice on 129 or B6 backgrounds, followed by staining for IgG (red) and DNA (blue), are shown. Representative of six animals per group (scale bars, 50 μm and in the inset 20 μm).

(B) Serum titers of anti-dsDNA IgG in WT or KO mice on the indicated backgrounds over time as determined by ELISA (individual animals and median).

(C) Serum titers of anti-dsDNA IgG subclasses in 40-week-old KO mice on the 129 background as measured by ELISA (individual animals and median).

(D and E) Anti-dsDNA IgG Ab-secreting cells (ASC) in WT and KO mice as determined by ELISPOT. ASC numbers per 5×10^5 splenocytes in 50-week-old (D) and 4- to 6-week-old (E) mice (individual animals and median) are shown.

(F) Serum titers of anti-nucleosome IgG in WT or KO mice on the 129 background as determined by ELISA (individual animals and median).

(G and H) Relative titers of anti-dsDNA and anti-nucleosome IgG in a synchronous cohort of KO mice analyzed over time. Titers are presented as a percent of the maximal value reached at any time point in each animal. The kinetics in three representative individual mice (G) and values in individual mice at 5 weeks (H) are shown. Significance is estimated by a paired Wilcoxon test.

Author Manuscript Author Manuscript Author Manuscript Author Manuscript

Statistical significance: *p ≤ 0.05; **p ≤ 0.01; ***p ≤ 0.001.
See also Figure S1.

Author Manuscript Author Manuscript Author Manuscript Author Manuscript

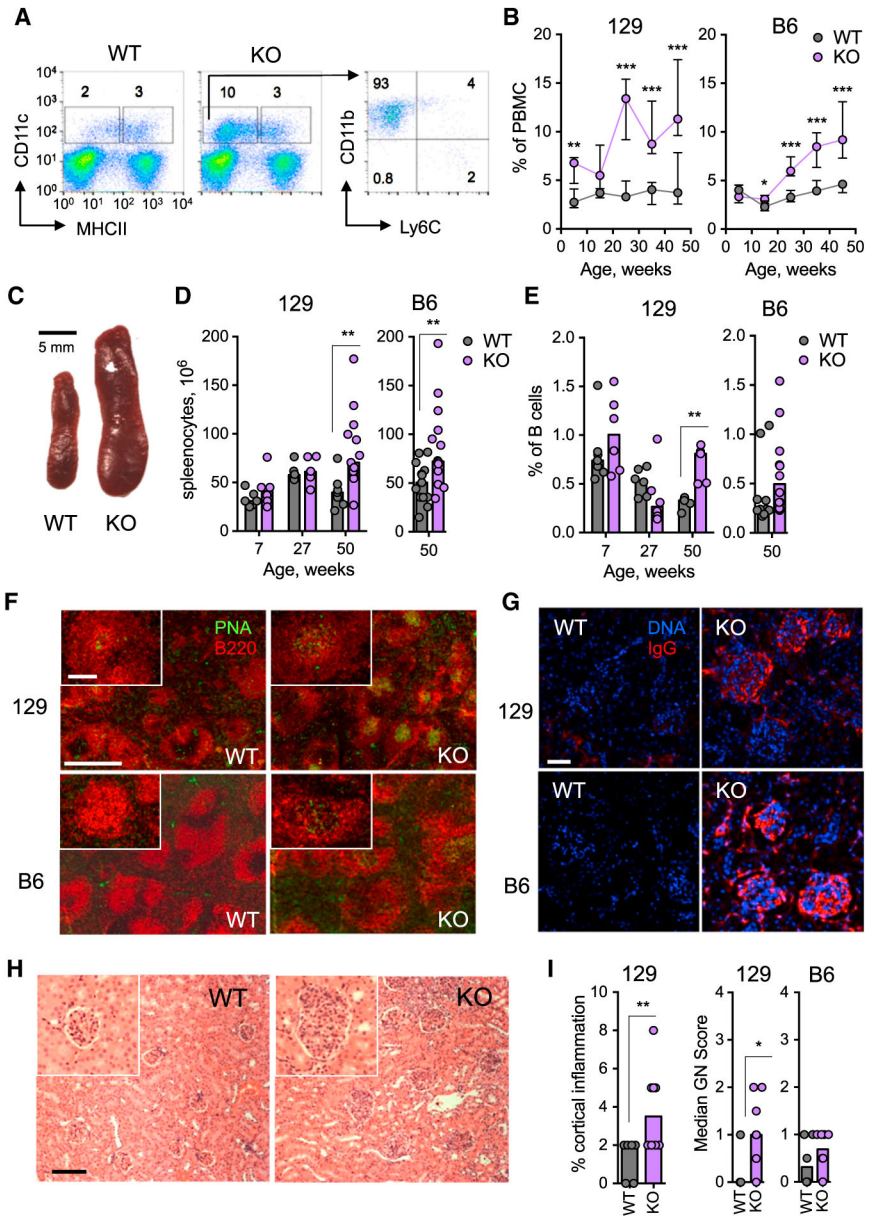

Figure 2. *Dnase1l3*-Deficient Mice Develop Late-Onset Immune Activation and Kidney Inflammation

(A and B) Monocyte population in the peripheral blood of *Dnase1l3* knockout (KO) and control wild-type (WT) mice. (A) Representative staining of peripheral blood mononuclear cells (PBMC) from WT and KO mice, with the fraction and phenotype of $CD11c^{+}$ MHC cl. II^{-} monocytes indicated.

(B) Fractions of $CD11c^{+}$ MHC cl. II^{-} monocytes among PBMC at the indicated time points (median ± interquartile range of nine animals per group).

(C) Representative spleens from WT and KO mice on a 129 background at 50 weeks of age.

(D) Absolute number of splenocytes in WT or KO mice at the indicated time points (individual animals and median).

Author Manuscript Author Manuscript Author Manuscript Author Manuscript

(E) The GCB cell population in the spleens of WT or KO mice at the indicated time points. The fractions of GC B cells ($B220^+$ PNA^+ $CD95^+$) among total $B220^+$ B cells (individual animals and median) are shown.

(F) The GC reaction in the spleens of WT or KO mice at 50 weeks of age. Splenic sections stained for total B cells (B220, red) and GC B cells (PNA, green; scale bar, 200 μm) with the individual GC in the inset (scale bar, 20 μm) are shown. Representative of six mice per genotype.

(G) IgG deposition in the kidneys of WT or KO mice at 50 weeks of age. Kidney sections stained for IgG (red) and DNA (blue) are shown. Representative of ten animals per group (scale bar, 50 μm).

(H) Kidney architecture in WT or KO mice on a 129 background at 50 weeks of age. Kidney sections stained with hematoxylin/eosin (scale bars, 50 μm) with a representative glomerulus in the inset are shown. Representative of eight animals per group.

(I) Histopathological score of glomerulonephritis in WT or KO mice at 50 weeks of age. The percentage of kidney cortex affected by inflammation and the median cumulative score of glomerulonephritis in mice on the indicated backgrounds are shown.

Statistical significance: *$p \leq 0.05$; **$p \leq 0.01$; ***$p \leq 0.001$.

See also Figure S2.

Author Manuscript Author Manuscript Author Manuscript Author Manuscript

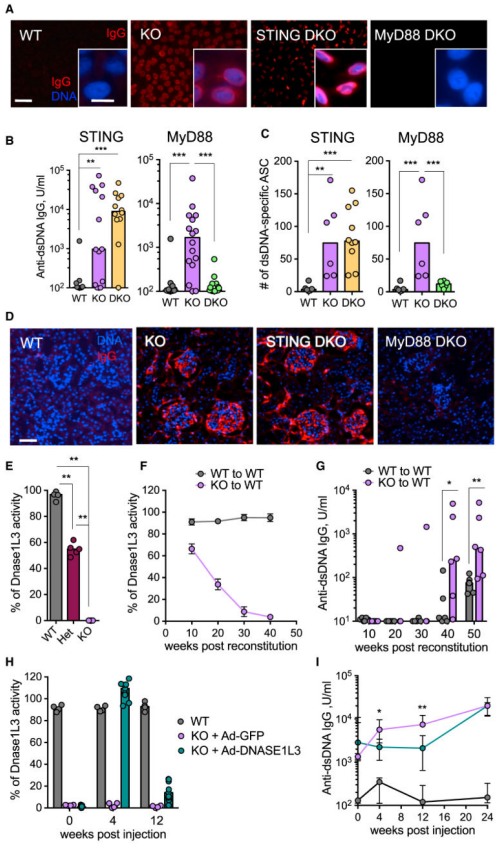

Figure 3. Autoreactivity in *Dnase1l3*-Deficient Mice Does Not Require STING and Is Restricted by Circulating DNASE1L3

(A–D) *Dnase1l3* knockout (KO) mice were crossed with STING-deficient or MyD88-deficient mice to generate double-KO (dKO) mice and analyzed along with the respective wild-type (WT) controls. (A) Serum ANA at 45 weeks of age. Results are shown as in Figure 1A; representative of six animals per group. (B) Serum titers of anti-dsDNA IgG at 35 weeks of age as determined by ELISA (individual animals and median). The difference between KO and STING dKO mice in the left panel is not statistically significant. (C) Anti-dsDNA IgG Ab-secreting cells (ASC) at 50 weeks of age as determined by ELISPOT. The numbers of ASC per 5×10^5 splenocytes (individual animals and median) are shown. (D) IgG deposition in the kidneys at 50 weeks of age. Results are shown as in Figure 2G; representative of five animals per group (scale bar, 50 μm).

(E) The relative activity of circulating DNASE1L3 in WT, KO, or heterozygous (Het) animals, as measured by the ability of serum to digest liposome-bound plasmid DNA (individual animals and median).

(F and G) WT recipients were lethally irradiated and reconstituted with WT or KO BM (KO-to-WT and control WT-to-WT chimeras, respectively). (F) Serum DNASE1L3 activity in chimeras at the indicated time points after reconstitution (mean ± SD of six animals per group). (G) Serum anti-dsDNA IgG titers at the indicated time points as measured by ELISA (individual animals and median).

(H and I) Autoreactivity in KO mice reconstituted with circulating DNASE1L3. Young 4-week-old KO mice were injected with adenoviruses encoding DNASE1L3 (Ad-DNASE1L3)

Author Manuscript Author Manuscript Author Manuscript Author Manuscript

or GFP (Ad-GFP). (H) Serum Dnase1L3 activity in KO mice administered Ad-DNASE1L3 or Ad-GFP at the indicated time points, along with age-matched wild-type controls (individual animals and median). (I) Serum anti-dsDNA IgG titers in the same mice as measured by ELISA. Data represent median ± a range of four (KO + Ad-GP) and nine (WT or KO + Ad-DNASE1L3) animals per group.

Statistical significance: *$p \leq 0.05$; **$p \leq 0.01$; ***$p \leq 0.001$.

See also Figure S3.

Author Manuscript Author Manuscript Author Manuscript Author Manuscript

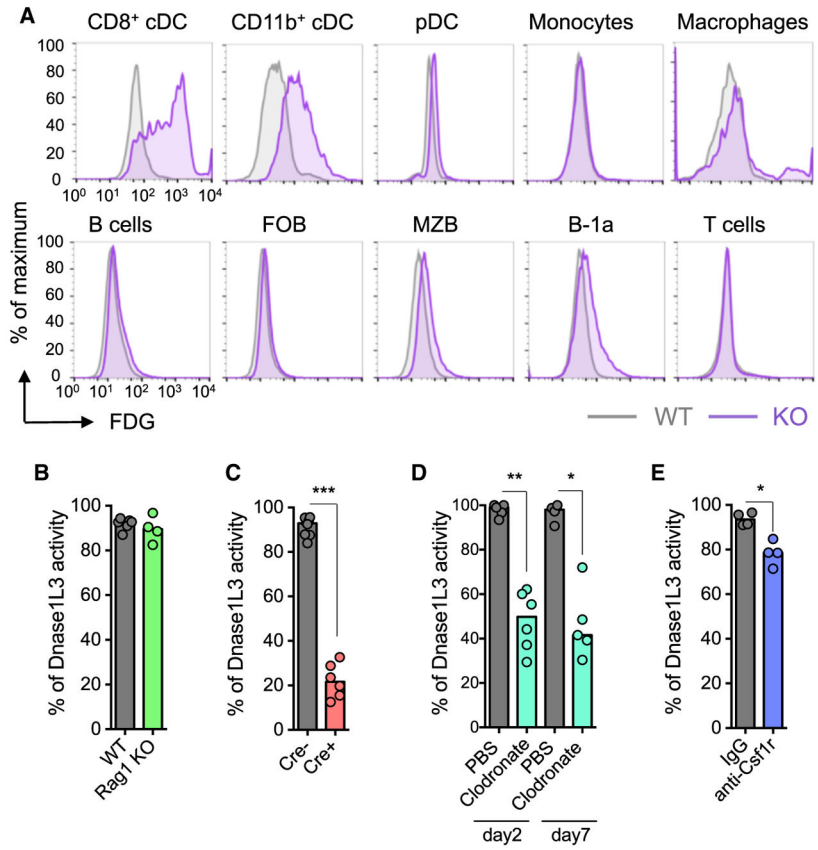

Figure 4. Circulating DNASE1L3 Is Produced Primarily by Dendritic Cells and Macrophages

(A) Single-cell analysis of Dnase1L3 expression in immune cells. Splenocytes from *Dnase1l3*$^{LacZ/LacZ}$ KO or WT control mice were stained for LacZ activity using the fluorescent substrate fluorescein di(β-D-galactopyranoside) (FDG). Histograms of FDG staining in the indicated gated cell populations (representative of three independent experiments) are shown. Similar results were obtained with heterozygous *Dnase1l3*$^{LacZ/+}$ mice (data not shown).

(B) Dnase1L3 activity in the sera of Rag1-deficient animals (individual animals and median).

(C) Dnase1L3 activity in the sera of DC-depleted animals. Animals with Cre-inducible diphtheria toxin receptor (DTR) with or without the DC-specific Cre deleter (CD11c-Cre) were administered diphtheria toxin (DTX) for 2 weeks, and their sera was analyzed for DNASE1L3 activity (individual animals and median).

(D) Dnase1L3 activity in the sera of wild-type animals treated with PBS- or clodronate-containing liposomes to deplete macrophages on the indicated days after treatment (individual animals and median).

(E) Dnase1L3 activity in the sera of wild-type animals 12 days after injection of control IgG or anti-Csf1r blocking Ab (individual animals and median).

Statistical significance: *p ≤ 0.05; **p ≤ 0.01; ***p ≤ 0.001.

See also Figure S4.

Author Manuscript Author Manuscript Author Manuscript Author Manuscript

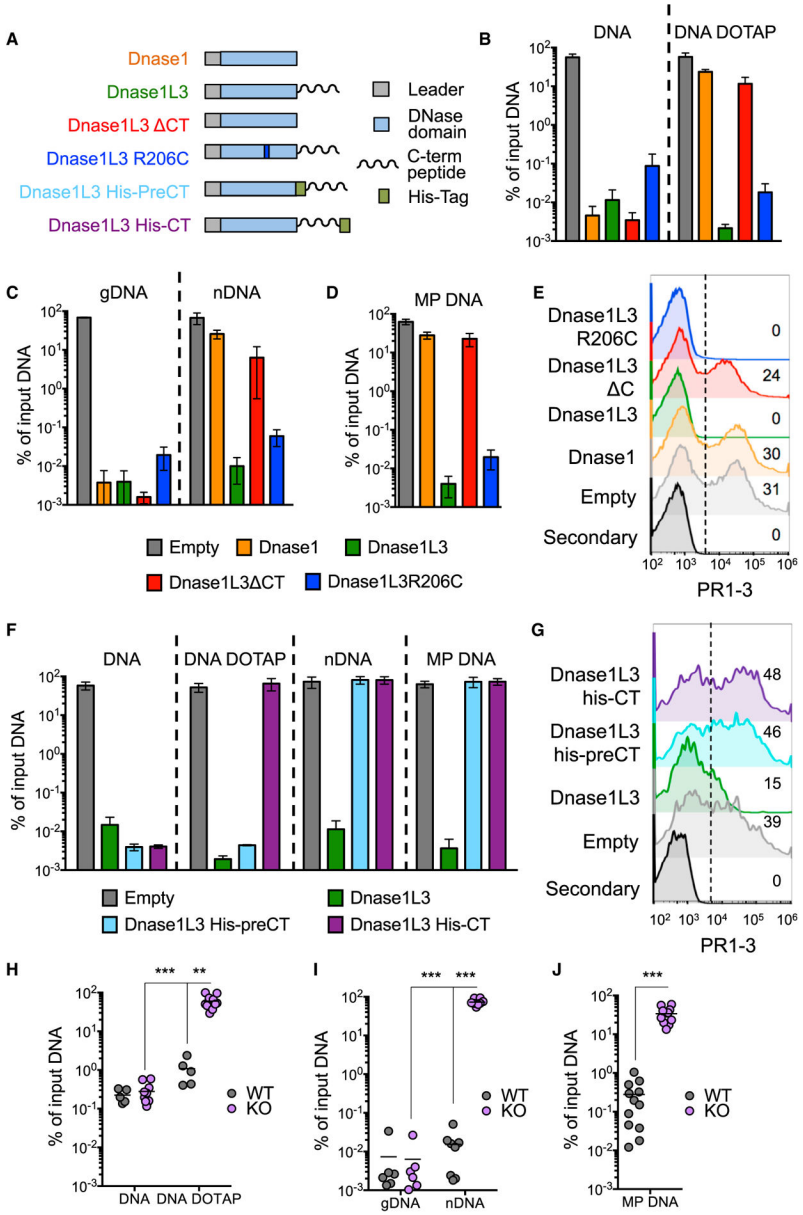

Figure 5. DNASE1L3 Can Digest Intact Chromatin and Genomic DNA in Apoptotic Microparticles

(A) Schematic of the different DNase constructs used.

(B–D) Digestion of different DNA substrates by recombinant DNases. DNA substrates were incubated with a control supernatant (empty, gray) or supernatants containing DNASE1, DNASE1L3, DNASE1L3's C-terminal truncation (DNASE1L3 ΔCT), or DNASE1L3's R206C substitution variant. The amount of remaining DNA was measured by qPCR and expressed as a percent of input DNA (mean ± SD of three independent experiments). (B) The digestion of plasmid DNA alone (DNA) or in complex with liposomal reagent (DNA DOTAP). (C) The digestion of purified human genomic DNA (gDNA) or purified human nucleosomes (nDNA).

Author Manuscript Author Manuscript Author Manuscript Author Manuscript

(D) The digestion of DNA within microparticles (MP) from apoptotic human cells (MP DNA).
(E) The digestion of chromatin on the surface of MP by recombinant DNases. MP from apoptotic human cells were incubated with recombinant DNases and stained with anti-nucleosome mAb PR1-3. Histograms of PR1-3 fluorescence and the percent of positive MP are shown; representative of three experiments.
(F) Digestion of DNA substrates by DNASE1L3 mutants with a hexahistidine tag at the C terminus (His-CT) or preceding it (His-preCT). DNA substrates and data presentation are as in (B)–(D).
(G) The digestion of chromatin on the surface of MP by hexahistidine-containing DNASE1L3 mutants. Data are presented as in (E).
(H–J) Digestion of different DNA substrates by sera from *Dnase1l3*-deficient knockout (KO) or control wild-type (WT) animals. The digestion of plasmid DNA with or without DOTAP (H), human purified or nucleosomal genomic DNA (I), or DNA within MP from apoptotic human cells (J) was measured as in (B)–(D). The results from sera of individual animals (circles) and median (lines) are shown.
Statistical significance: $^{**}p \leq 0.01$; $^{***}p \leq 0.001$.
See also Figure S5.

Author Manuscript Author Manuscript Author Manuscript Author Manuscript

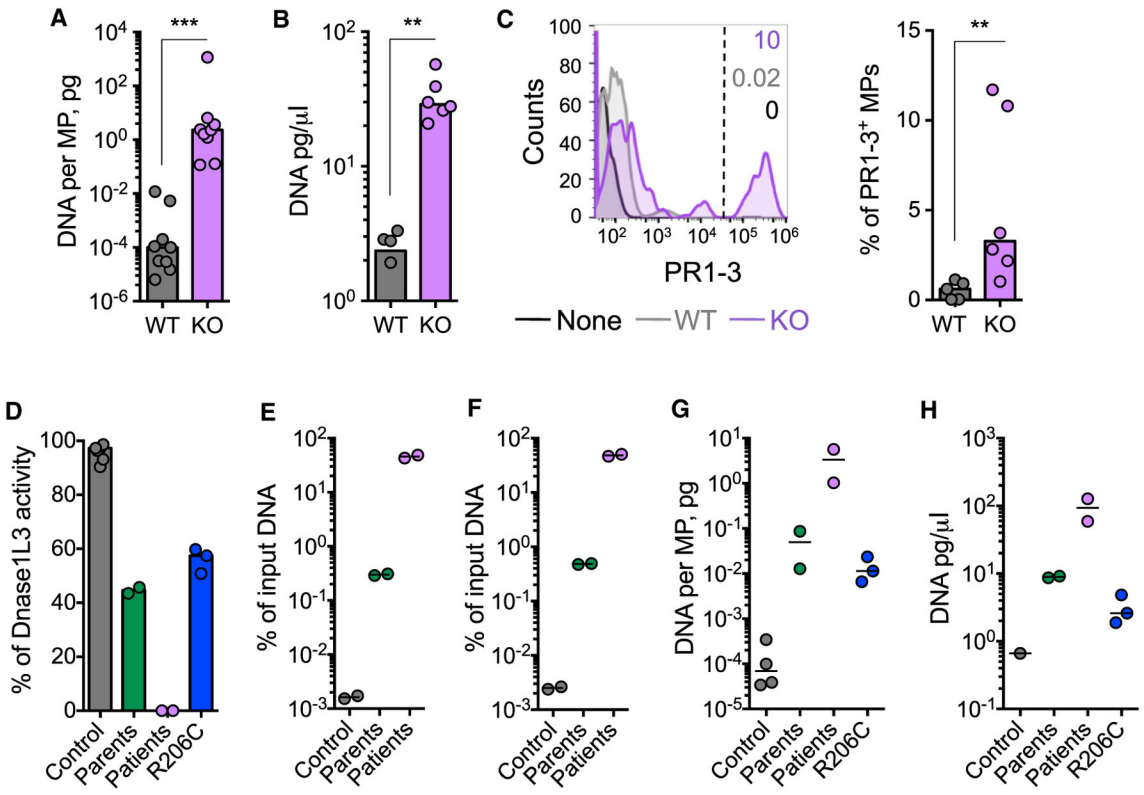

Figure 6. DNASE1L3 Deficiency in Mice and Human Patients Causes the Accumulation of DNA in Circulating Microparticles

(A) The genomic DNA cargo of circulating microparticles (MP) from *Dnase1l3* knockout (KO) or control wild-type (WT) animals. MP were isolated from the plasma of 10-week-old mice and analyzed by qPCR for mouse genomic DNA. Results show the amount of DNA per MP in individual mice (circles) and group median (bar).

(B) The amount of genomic DNA per volume of unfractionated plasma from WT and KO animals (individual animals and median).

(C) The binding of anti-nucleosome mAb PR1-3 to circulating MP isolated from the plasma of young KO or WT mice. Representative histograms of PR1-3 fluorescence and the frequency of positive MP (individual animals and median) are shown.

(D–H) Plasma from human *DNASE1L3*-deficient patients (n = 2), their haplodeficient parents (n = 2), individuals with the DNASE1L3 R206C polymorphism (n = 3), and normal control subjects (n = 2–5) were analyzed. Data represent individual human subjects and the median (bar or line). (D) DNASE1L3 activity in the soluble fraction of patients' plasma, measured using the digestion of DOTAP-coated plasmid DNA and expressed as a percent of the activity in a reference control plasma. (E) The digestion of human nucleosomes by the soluble fraction of patients' plasma. (F) The digestion of DNA in MP from apoptotic human cells by the soluble fraction of patients' plasma. (G) The amount of genomic DNA in circulating MP isolated from the plasma. Results show the amount of DNA per MP as determined by qPCR for human genomic DNA. (H) The amount of genomic DNA per volume of unfractionated plasma as determined by qPCR.

Statistical significance: $^{**}p \leq 0.01$; $^{***}p \leq 0.001$.

Author Manuscript Author Manuscript Author Manuscript Author Manuscript

See also Figure S6.

Author Manuscript Author Manuscript Author Manuscript Author Manuscript

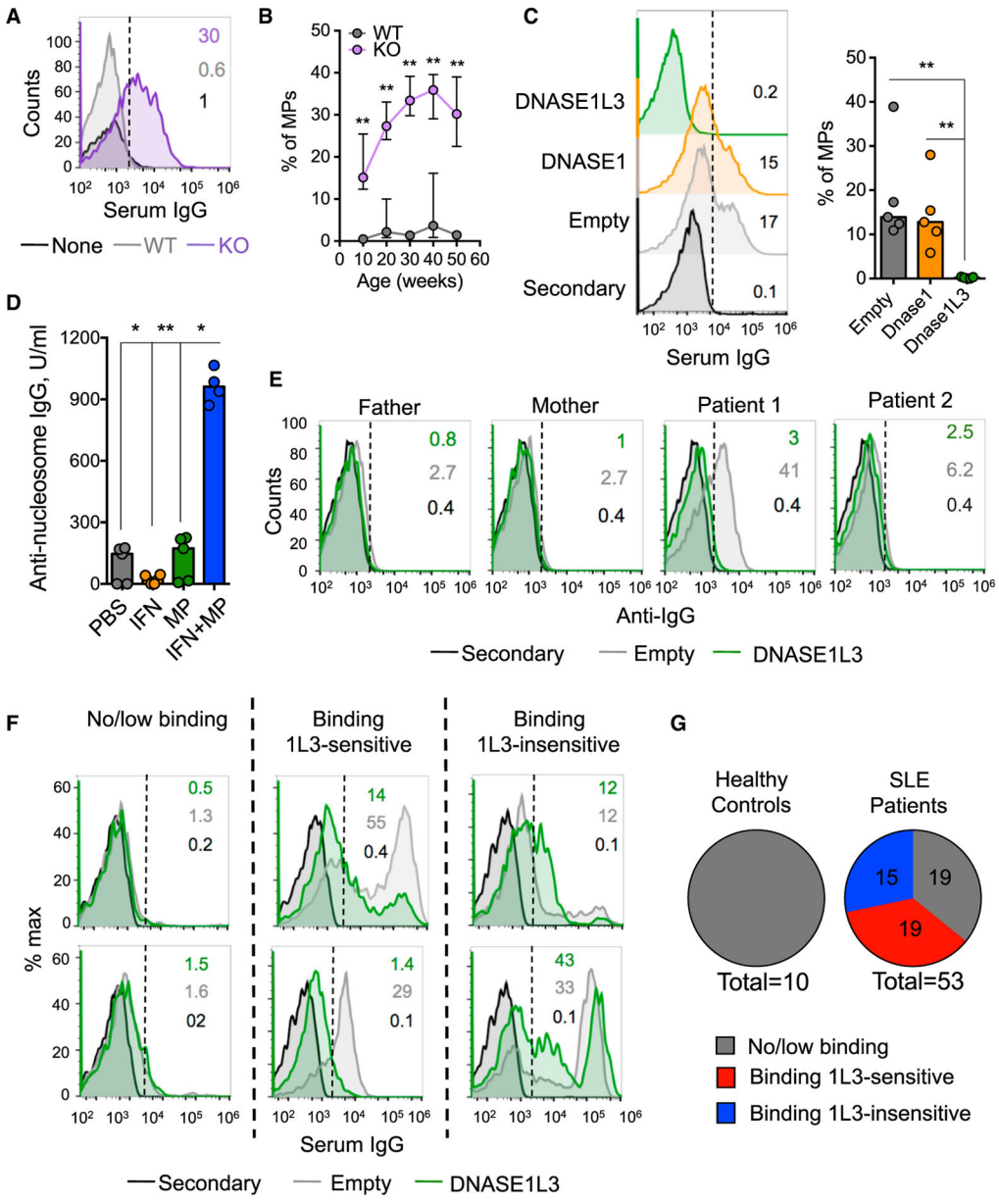

Figure 7. DNASE1L3-Sensitive Chromatin on Apoptotic Microparticles Is Antigenic in Mice and Human Patients

(A–C) Binding of mouse serum IgG to the surface of microparticles (MP). Human apoptotic MP were incubated with sera from *Dnase1l3* knockout (KO) or control wild-type (WT) animals, followed by secondary anti-mouse IgG Ab. (A) Representative histograms of IgG fluorescence and the percent of positive MP. (B) Fractions of IgG-positive MP stained with sera from WT or KO mice of the indicated ages (median ± range of five animals per group). (C) MP were incubated with supernatants containing human DNASE1, DNASE1L3, or an empty control prior to staining with KO serum. Representative histograms of IgG fluorescence and the frequency of positive MP stained by sera from individual KO mice (bars represent the median) are shown. Statistical significance: *p≤0.05; **p≤0.01; ***p ≤ 0.001.

Author Manuscript Author Manuscript Author Manuscript Author Manuscript

(D) Anti-nucleosome response in the animals immunized with MP. Wild-type mice were administered IFN-α adenovirus (IFN), MP from syngeneic apoptotic splenocytes (MP), or both, and serum IgG to nucleosomes were measured by ELISA 1 week after the last MP immunization. Titers from individual animals (circles) and median titers (bars) are shown. (E–G) DNASE1L3-sensitive binding of IgG from human patients to the surface of MP. Human apoptotic MP were treated with DNASE1L3-containing supernatant (DNASE1L3) or a control supernatant (empty), incubated with plasma from human subjects, followed by secondary anti-human IgG Ab. Representative histograms of IgG fluorescence and the percent of positive MP are shown. (E) DNASE1L3-sensitive binding of IgG from *DNASE1L3*-deficient patients or their haplodeficient parents. Representative histograms of IgG fluorescence and the percent of positive MP are shown. (F) DNASE1L3-sensitive binding of IgG from patients with sporadic SLE. Two representative histograms of IgG fluorescence for each reactivity pattern are shown. (G) The fraction of SLE patients with the reactivity patterns are shown in (F).
See also Figure S7.